Journal of Power Sources 185 (2008) 1589–1593

Contents lists available at ScienceDirect

Journal of Power Sources

journal homepage: www.elsevier.com/locate/jpowsour

Short communication

Composite electrode composed of bimodal porous carbon and polypyrrole for electrochemical capacitors

Sang-Wook Woo [a], Kaoru Dokko [b,*], Kiyoshi Kanamura [a]

[a] Department of Applied Chemistry, Tokyo Metropolitan University, 1-1 Minami-ohsawa, Hachioji, Tokyo 192-0397, Japan
[b] Department of Chemistry and Biotechnology, Yokohama National University, 79-5 Tokiwadai, Hodogaya-ku, Yokohama 240-8501, Japan

ARTICLE INFO

Article history:
Received 6 August 2008
Received in revised form 19 August 2008
Accepted 19 August 2008
Available online 23 August 2008

Keywords:
Colloidal crystal template
Macroporous carbon
Polypyrrole
Electrochemical capacitors

ABSTRACT

Three-dimensionally ordered macroporous (3DOM) carbons having walls composed of mesosized spherical pores were prepared by a colloidal crystal templating method. A composite electrode consisting of bimodal porous carbon and polypyrrole (PPy) was prepared by electropolymerization of pyrrole within the macropores of the bimodal porous carbon. The porous structure of the composite electrode was analyzed using a scanning electron microscope and by nitrogen adsorption–desorption measurement. It was found that the deposition of PPy decreased the porosity and specific surface area of the electrode. The electrochemical properties of the composite electrode were characterized in a mixed solution of ethylene carbonate and diethyl carbonate containing 1 mol dm^{-3} $LiPF_6$. The discharge capacity of the carbon–PPy composite electrode was 78 mAh $g_{carbon-PPy}{}^{-1}$ in the potential range of 2.0–4.0 V vs. Li/Li^+, which corresponded to a volumetric discharge capacity of 53 mAh cm^{-3}. Both the double-layer capacity (31 mAh g^{-1}) and the redox capacity of PPy (47 mAh g^{-1}) contributed to the discharge capacity of the composite electrode. This indicates that the incorporation of PPy into the macropores of bimodal porous carbon is effective in increasing the volumetric discharge capacity of the composite electrode. The composite of carbon and PPy showed good rate capability, and its discharge capacity at a high current density of 4.0 A g^{-1} was as high as 49 mAh g^{-1}.

1. Introduction

Rechargeable lithium batteries and electrochemical capacitors have been developed as power sources for portable electronic devices, electric vehicles (EVs), plug-in hybrid electric vehicles, and so on. In these electrochemical devices, porous electrodes consisting of an active material, polymer binder, and conductive agent have been used to increase the electrochemical interface. The electrode materials and the electrode structure have been intensively studied to improve the energy density and power density of energy storage devices. In these devices, the electrochemical reactions take place at the interface and the reaction rate strongly depends on the nature of the interface, which is composed of the electrode and electrolyte. A large electrochemical interface is favorable to increase the power density of energy storage devices. Therefore, the characteristics of the porous electrodes, such as the specific surface area (SSA), porosity, and pore size distribution (PSD), are key parameters to determine the performance of electrochemical devices.

One of the interesting technologies used to fabricate porous electrodes is the colloidal crystal templating method. Three-dimensionally ordered macroporous (3DOM) materials can be prepared by this method, and these materials have been intensively studied in various fields, such as catalysts [1], biomaterials [2], photonics [3], and sensors [4]. Recently, we successfully prepared 3DOM carbon having walls composed of mesosized pores [5]. The prepared bimodal porous carbons were investigated as electrode materials for lithium-ion capacitors and electric double-layer capacitors [6,7]. However, this kind of porous carbon has a drawback with regard to its practical use, because a high electrode porosity causes a decrease in the volumetric energy density of energy storage devices.

Bimodal porous carbon has a high porosity, and redox active materials can be incorporated into its macropores. The incorporation of active materials such as transition metal oxides [8–10] and conducting polymers [11–15] will increase the volumetric charge and discharge capacities of porous carbon. In this work, a composite electrode consisting of bimodal porous carbon and polypyrrole (PPy) was prepared by the electropolymerization of pyrrole within the macropores of bimodal porous carbon. The electrochemical properties of the prepared composite were examined in a non-

* Corresponding author. Tel.: +81 45 339 3942; fax: +81 45 339 3942.
E-mail address: dokko@ynu.ac.jp (K. Dokko).

0378-7753/$ – see front matter © 2008 Elsevier B.V. All rights reserved.
doi:10.1016/j.jpowsour.2008.08.035

aqueous electrolyte as a positive electrode for electrochemical capacitors.

2. Experimental

Bimodal porous carbon, which is 3DOM carbon with walls composed of spherical mesopores, was prepared by the colloidal crystal templating method. Polystyrene (PS) latex and colloidal silica were utilized to prepare the colloidal crystal templates for the bimodal porous carbon. PS particles with a diameter of 204 nm, purchased from Seradyn Inc., were utilized as the template for the macropores. Colloidal silica SC15 (Snowtex®, supplied by Nissan Chemical Industries Ltd.), with diameters of 10–20 nm, was used as the template for the mesopores. Mono-dispersed PS latex and the colloidal silica particles were uniformly mixed in deionized water by ultrasonic treatment. The water in the mixed suspension was simply evaporated in a Petri dish at 333 K for 24 h, and the PS–silica composite was accumulated at the bottom of the Petri dish. The volume ratio of PS to silica in the composite was controlled at 74:26, which allowed the PS beads to form a close-packed lattice in the composite. The obtained PS–silica composites were treated at high temperatures in a horizontal furnace under dry argon flow (40 mL min^{-1}), in order to carbonize the PS beads. The temperature was increased from room temperature to 1273 K at a heating rate of 4 K min^{-1} and it was then reduced to room temperature. After the carbonization, the silica particles were removed with 20% aqueous hydrofluoric acid, and the resulting porous carbons were washed with ultra pure water and dried in a vacuum oven at 383 K.

The porous carbon electrode was prepared by mixing bimodal porous carbon and polytetrafluoroethylene (PTFE) binder in a weight ratio of 90:10. This mixture was rolled into a thin sheet of uniform thickness and cut into a circular sheet with a diameter of 13 mm. This sheet was then pressed on a titanium mesh current collector. The thickness of the sheet was 130–135 μm at this point, and the mass of the bimodal porous carbon in the sheet was 5.5 mg. Electrochemical polymerization of pyrrole on the porous carbon electrode was carried out by a cyclic potential sweep in a propylene carbonate (PC) solution containing 1.0 mol dm^{-3} $LiClO_4$ and 0.2 mol dm^{-3} pyrrole. A conventional three-electrode cell was utilized for the polymerization, and Li/Li^+ (1 mol dm^{-3} $LiClO_4$ in PC) and an activated carbon electrode (KYNOL™, BET-SSA: 2000 m^2 g^{-1}) were used as the reference and counter electrodes, respectively. The prepared composite electrode was rinsed in ethanol to remove pyrrole monomer, and dried under vacuum at 363 K for 1 day. The composite electrode is hereafter denoted as carbon–PPy(x) (x: content of PPy), for example, carbon–PPy(60) denotes that the composite was composed of 40 wt% carbon and 60 wt% PPy.

The porous structure of the composite electrode was observed using a field-emission scanning electron microscope (FE-SEM, JSM 6700F, JEOL). Nitrogen (N_2) adsorption–desorption measurement at 77 K was conducted using a porosimetry analyzer (Belsorp-mini II, BEL Japan Inc.). The specific surface area (S_{BET}) was calculated from the Brunauer–Emmett–Teller (BET) plot of the nitrogen adsorption isotherm. The pore size distribution and average pore diameter (D_{BJH}) in the range of 2–50 nm were calculated by using the Barret–Joyner–Halenda (BJH) method with the adsorption branch of the N_2 isotherm [16]. The surface area (S_{micro}) and pore volume (V_{micro}) of the micropores of the prepared carbon and composite were estimated by the t-plot method [17].

A standard three-electrode electrochemical cell was assembled to measure the specific capacity of the carbon–PPy composite electrode. The counter electrode was activated carbon fiber, and Li/Li^+, $LiClO_4$ (1 mol dm^{-3} $LiClO_4$ in PC) was used as the reference electrode. A mixed solution of ethylene carbonate (EC) and diethyl carbonate (DEC) containing 1.0 mol dm^{-3} $LiPF_6$ was used as the electrolyte. Cyclic voltammetry was carried out using an automatic polarization system (HZ-100R, Hokuto Denko). A galvanostatic discharge–charge test was performed using an automatic discharge–charge instrument (HJR-110mSM6, Hokuto Denko). All electrochemical measurements were carried out in an argon-filled grove box at room temperature.

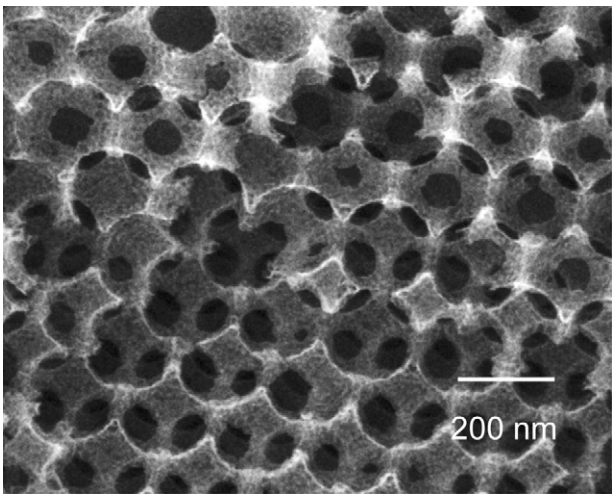

Fig. 1. FE-SEM of bimodal porous carbon.

3. Results and discussion

Fig. 1 shows the FE-SEM images of the prepared bimodal porous carbon. The formation mechanism of the bimodal porous structure has been reported elsewhere [7]. During the evaporation of water in the mixed suspension of PS and silica, the mono-dispersed PS beads were self-assembled into an ordered lattice, wherein the silica particles were forced to pack closely at the interstices between the PS beads [5–7]. Heat treatment of the PS–silica composite created 3D-ordered macropores owing to the decomposition of PS, and simultaneously, some fragments of the decomposing polymer deposit were formed around the silica colloids. Finally, the removal

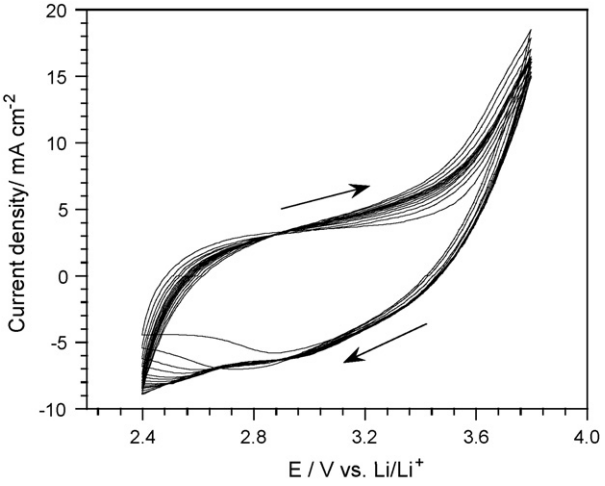

Fig. 2. Cyclic voltammograms bimodal porous carbon electrode in a propylene carbonate solution containing 1.0 mol dm^{-3} $LiClO_4$ and 0.2 mol dm^{-3} pyrrole. The potential sweep rate was 10 mV s^{-1}, and potential sweep was carried out successively 15 cycles.

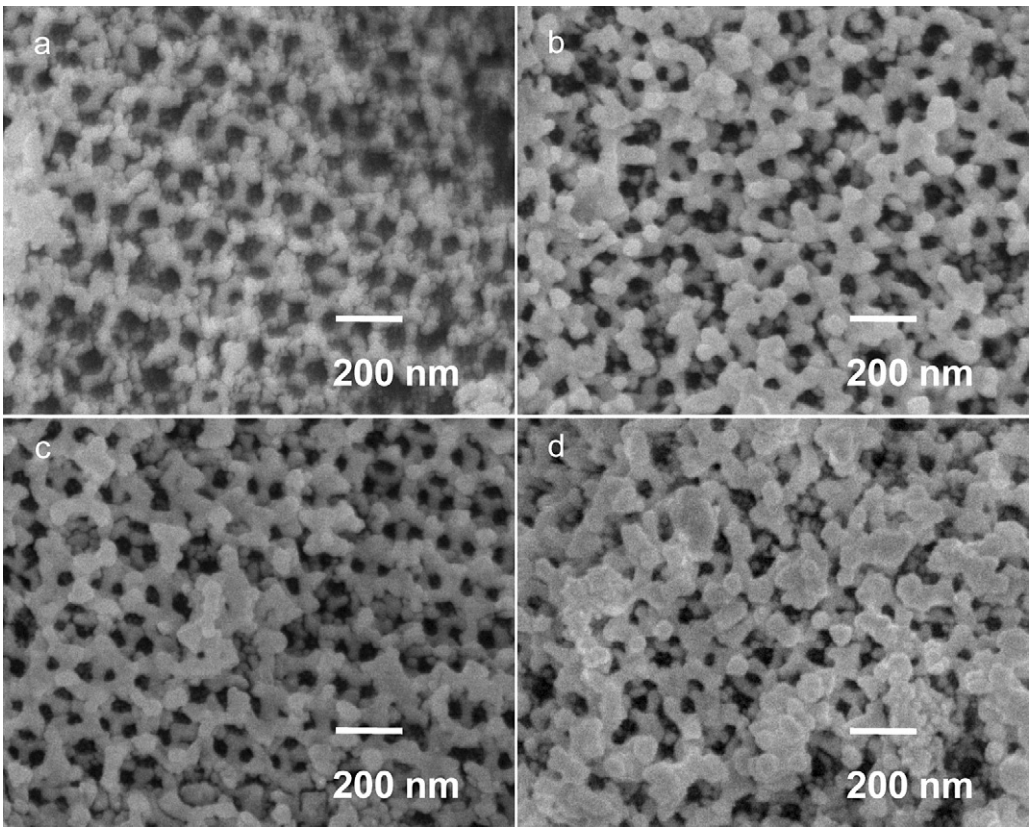

Fig. 3. FE-SEM images of composite electrodes consisting of bimodal porous carbon and PPy. The contents of PPy in the composite electrodes were 37.6 wt% (a), 52.5 wt% (b), 57.4 wt% (c), and 61.9 wt% (d), respectively.

of silica particles by HF etching created mesopores, and bimodal porous carbon was obtained. The prepared carbon had an inverse opal structure, and then, the macropore size (190 nm) was slightly smaller than the size of the PS bead (204 nm) used as the template for the macropores. This is probably due to the shrinkage of the macropore during the carbonization process. As shown in Fig. 1, the wall of the macropore was composed of spherical mesopores, and the mesopore size, 10–20 nm, showed good agreement with the size of the silica particle used as the template for the mesopores.

Electrochemical polymerization of pyrrole on the bimodal porous carbon was conducted by cyclic potential sweep in a PC solution containing pyrrole [18,19]. Fig. 2 shows the cyclic voltammograms (CVs) of porous carbon in the PC solution containing pyrrole. In the first cycle, a large anodic current was observed at above 3.5 V vs. Li/Li^+, indicating the formation of radical cations by the electrochemical oxidation of pyrrole [20]. These radical cations were transient intermediates and they were coupled with each other, resulting in the formation of PPy. As a result of PPy formation, the redox currents corresponding to the doping and undoping of ClO_4^- anions gradually increased with the cycle number [18,19]. Fig. 3 shows the SEM images of the carbon–PPy composite electrodes. PPy was deposited on the surface of the macropores, and the porosity of the carbon gradually decreased with an increase in the cycle number. After 22 cycles of the potential sweep, PPy occupied the most of macropores in the porous carbon. This resulted in the blockage of the connecting windows between the macropores. The PPy deposited after 22 cycles accounted for about 62 wt% in the composite.

The pore size distribution of the bimodal porous carbon is shown in Fig. 4(a). It is clear that the bimodal porous carbon has mesopores ranging in size from 10 to 20 nm. The mesopore size centered at around 12 nm is in good agreement with the silica particle size (10–20 nm diameter) used as the template. The increase in the pore volume corresponding to a pore size of around 2 nm is probably due to the interstitial space between the spherical mesopores. Fig. 4(b) shows the PSD of carbon–PPy(57). The deposition of PPy decreased the peak diameter of the mesopores, indicating that the mesopores of the bimodal porous carbon were partly filled with PPy. The pore characteristics of the bimodal porous carbon and the carbon–PPy

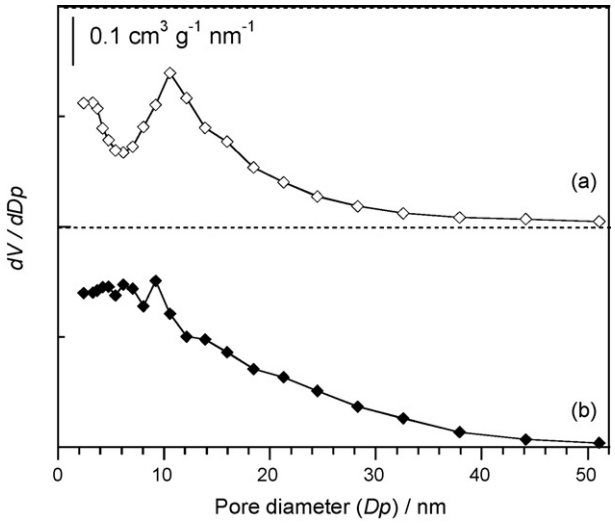

Fig. 4. Pore size distributions of bimodal porous carbon (a) and carbon–PPy composite (57 wt%) (b).

Table 1
The pore characteristics of bimodal porous carbon and carbon–PPy (57.4 wt%) composite

Item	Specific surface areas ($m^2\ g^{-1}$)			Pore diameter (nm)		Pore volume ($cm^3\ g^{-1}$)	
	S_{BET} [a]	S_{micro} [b]	S_{ext} [c]	D_{BJH} [d]	D_{macro} [e]	V_{total} [f]	V_{micro} [g]
Bimodal porous carbon	1018	63	955	13	190	2.97	0.023
Carbon–PPy (57.4 wt%)	262	25	236	9	–	0.58	0.010

[a] BET surface area.
[b] Micropore surface area calculated from *t*-polt method.
[c] External surface area ($S_{ext} = S_{BET} - S_{micro}$).
[d] Average pore diameter calculated from BJH method.
[e] Pore diameter estimated from SEM observation.
[f] Total pore volume at a relative pressure of 0.99.
[g] Micropore volume calculated from *t*-plot method.

composite are summarized in Table 1. The BET-SSA (S_{BET}) of the bimodal porous carbon was found to be 1020 $m^2\ g^{-1}$. The surface area of the micropores (<2 nm) estimated by the *t*-plot method was less than 10% of BET-SSA. Therefore, both the mesopores and macropores were the major contributors to the surface area of the porous carbon. On the other hand, the BET-SSA of the carbon–PPy composite was about 262 $m^2\ g^{-1}$. The introduction of PPy into the bimodal porous carbon resulted in a significant decrease in the SSA and the total pore volume (V_{total}).

Fig. 5 displays the CVs of the carbon–PPy composite electrodes in 1 mol dm^{-3} $LiPF_6$ (EC + DEC) at a scan rate of 5 mV s^{-1}. The initial potentials (immersion potentials of the electrode) of the bare porous carbon and carbon–PPy were between 3.0 and 3.3 V vs. Li/Li^+. The bare porous carbon electrode showed a rectangle-like shape corresponding to the typical profile of a double-layer capacitor in the voltammograms [21]. From the shape of the CV curve for the bare porous carbon, it was evident that a Faradaic process is hardly involved in the potential range of 2.0–4.0 V vs. Li/Li^+. In the case of the composite electrodes consisting of the porous carbon and PPy, besides the current response due to the formation of an electric double layer, a redox current response was observed in the potential range of 2.4–4.0 V. In this potential region, doping/undoping of PF_6^- anion into/from PPy took place [22–26]. In the PPy content range of 0–60 wt%, the redox currents increased with the PPy content. Despite the large amount of PPy, the redox current of the carbon–PPy(62) electrode was smaller than that of carbon–PPy(57). In the case of carbon–PPy(62), the blockage of the connecting windows between the macropores occurred during the electropolymerization process, as shown in Fig. 3(d), and this hindered ionic conduction within the composite electrode. This would have led to the increase in the electrode resistance and decrease in the redox capacity of the electrode.

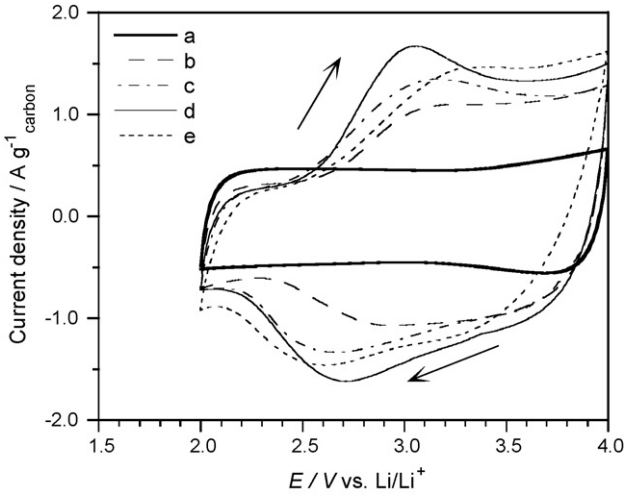

Fig. 5. Cyclic voltammograms of bimodal porous carbon (a) and carbon–PPy composite electrodes (b–e) measured at a scan rate of 5 mV s^{-1} in an electrolyte of 1 mol dm^{-3} $LiPF_6$/EC + DEC. The contents of PPy in the composite electrodes were 49.0 wt% (b), 54.6 wt% (c), 57.4 wt% (d), and 61.9 wt% (e), respectively. The current of cyclic voltammogram was normalized by the mass of bimodal porous carbon in the composite electrode.

Fig. 6 shows the charge and discharge curves of the bare porous carbon and carbon–PPy(57) measured at a current density of 0.1 A g^{-1} in 1 mol dm^{-3} $LiPF_6$ (EC + DEC). The electrode potential of the bare porous carbon changed linearly with the quantity of electricity passed in the charging and discharging processes. This can be attributed to the charging and discharging of the electric double layer and is in good agreement with the result of cyclic voltammetry. In contrast, the charge and discharge curves of carbon–PPy(57) exhibited an inflection at around 2.4 V. In the potential range of 2.0–2.4 V, charging and discharging of the double layer took place, while the Faradaic process hardly occurred. Besides the double-layer formation, doping/undoping of PF_6^- anion into/from PPy took place in the potential range of 2.4–4.0 V. The discharge capacities of the bare porous carbon and carbon–PPy(57) measured at a current density of 0.1 A g^{-1} were 53 mAh g_{cabon}^{-1} and 78 mAh $g_{carbon-PPy}^{-1}$, respectively. Thus, the incorporation of PPy dramatically increased the charge storage capacity of the electrode. The discharge capacity of carbon–PPy(57) was attributed to the sum of the discharge capacity of the electric double layer (31 mAh $g_{carbon-PPy}^{-1}$) and the redox capacity (47 mAh $g_{carbon-PPy}^{-1}$). The discharge capacity due to the redox of PPy can be calculated as 81 mAh g_{PPy}^{-1} based on the mass of the deposited PPy, corresponding to a doping level of 0.3 electrons per pyrrole unit. The volumetric capacity of the composite was found to be 53 mAh cm^{-3}, which is three times larger than that of the bare porous carbon (17 mAh cm^{-3}). The porosity of the bare

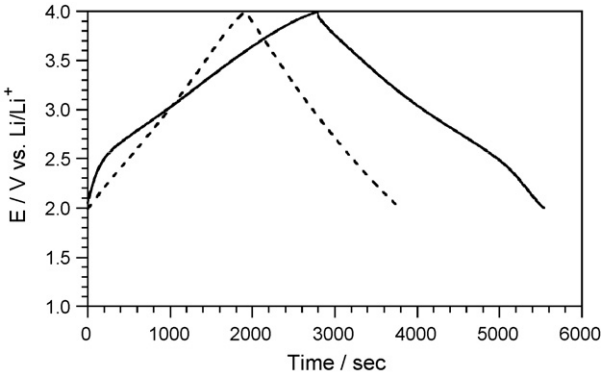

Fig. 6. Charge and discharge curves of bimodal porous carbon (dash line) and carbon–PPy (57.4 wt%) composite electrode (solid line) measured at the current density of 0.1 A g^{-1} in an electrolyte of 1 mol dm^{-3} $LiPF_6$/EC + DEC.

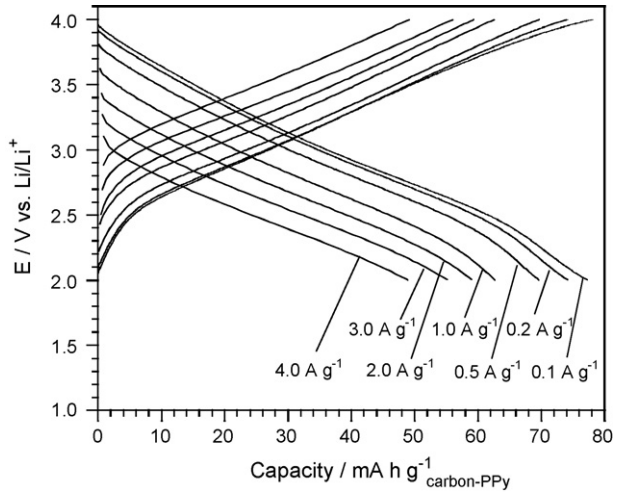

Fig. 7. Charge and discharge curves of the carbon–PPy (57.4 wt%) composite electrode measured at various current densities.

bimodal porous carbon was more than 70%, and the incorporation of PPy into the macropores did not change the geometric volume of the carbon electrode. Therefore, this kind of macroporous structure is suitable to support electrochemically active materials.

Fig. 7 shows the charge and discharge curves of carbon–PPy(57) measured at various current densities. As mentioned above, the discharge capacity of carbon–PPy(57) measured at a low current density of 0.1 A g^{-1} was 78 mAh g^{-1}, and the current density of 78 mA g^{-1} was defined as 1 C rate. Although the charge and discharge capacities decreased gradually as increasing the current density, the composite of carbon and PPy showed good rate capability. The discharge capacity obtained at a high current density of 4.0 A g^{-1} (50 C rate) was as high as 49 mAh g^{-1}, which is 62% of the discharge capacity of 78 mAh g^{-1} measured at a low current density of 0.1 A g^{-1}. The gravimetric current density of 4.0 A g^{-1} corresponds to the geometric current density of 19.4 mA cm^{-2} for the composite electrode. The rate capability of carbon–PPy(57) in a non-aqueous electrolyte is good compared with those of electrically conducting polymer–carbon composite electrodes presented in the literature [27,28]. The high rate capability of the carbon–PPy composite prepared in this work can be attributed to the facile doping/undoping process at the large interface between PPy and the electrolyte in the composite electrode.

4. Conclusions

We prepared bimodal porous carbon by a colloidal crystal templating method. A composite electrode consisting of bimodal porous carbon and PPy was prepared by the electropolymerization of pyrrole within the macropores of the bimodal porous carbon. The deposition of PPy decreased the porosity of the electrode, and the optimum amount of PPy in the composite electrode was 57 wt%, which could deliver the maximum discharge capacity. The discharge capacity of the carbon–PPy composite electrode was 78 mAh $g_{carbon-PPy}{}^{-1}$ in the potential range of 2.0 and 4.0 V vs. Li/Li^+, which corresponded to a volumetric discharge capacity of 53 mAh cm^{-3}, and the double-layer capacity (31 mAh g^{-1}) and redox capacity of PPy (47 mAh g^{-1}) contributed to the discharge capacity of the composite electrode. The incorporation of PPy into the macropores of the bimodal porous carbon was effective in increasing the volumetric discharge capacity of the composite electrode. The composite of carbon and PPy showed good rate capability, and its discharge capacity at a high current density of 4.0 A g^{-1} was as high as 49 mAh g^{-1}.

Acknowledgements

This work was partially supported by the Industrial Technology Research Grant Program in 2007 (07A22007a) from the New Energy and Industrial Technology Development Organization (NEDO) of Japan. The authors thank Prof. Hideki Masuda and Dr. Kazuyuki Nishio (Tokyo Metropolitan University) for their kind help in taking the FE-SEM photographs.

References

[1] Z. Wang, F. Hu, P.K. Shen, Electrochem. Commun. 8 (2006) 1764.
[2] C.J. Buchko, K.M. Kozoloff, D.C. Matrin, Biomaterials 22 (2001) 1289.
[3] M.W. Perpall, K.P.U. Perera, J. Dimaio, J. Ballato, S.H. Foulger, D.W. Smith Jr., Langmuir 19 (2003) 7153.
[4] J.H. Holtz, S.A. Asher, Nature 389 (1997) 7153.
[5] S.W. Woo, K. Dokko, K. Sasajima, T. Takei, K. Kanamura, Chem. Commun. (2006) 4099.
[6] S.W. Woo, K. Dokko, H. Nakano, K. Kanamura, Electrochemistry 75 (2007) 635.
[7] S.W. Woo, K. Dokko, H. Nakano, K. Kanamura, J. Mater. Chem. 18 (2008) 1674.
[8] H. Yamada, K. Tagawa, M. Komatsu, I. Moriguchi, T. Kudo, J. Phys. Chem. C 111 (2007) 8397.
[9] S.R. Sivakkumar, J.M. Ko, D.Y. Kim, B.C. Kim, G.G. Wallace, Electrochim. Acta 52 (2007) 7377.
[10] D. Bélanger, T. Brousse, J.W. Long, Electrochem. Soc. Interface 17 (1) (2008) 49.
[11] P. Novak, K. Muller, K.S.V. Santhanam, O. Hass, Chem. Rev. 97 (1997) 207.
[12] K. Naoi, M. Morita, Electrochem. Soc. Interface 17 (1) (2008) 44.
[13] V. Khomenko, E. Frackowiak, F. Beguin, Electrochim. Acta 50 (2005) 2499.
[14] V. Gupta, N. Miura, Electrochim. Acta 52 (2006) 1721.
[15] M.J. Bleda-Martínez, C. Peng, S. Zhang, G.Z. Chen, E. Morallón, D. Cazorla-Amorósa, J. Electrochem. Soc. 155 (2008) A672.
[16] E.P. Barrett, L.G. Joyner, P.P. Halenda, J. Am. Chem. Soc. 73 (1951) 373.
[17] F. Rouquerol, J. Rouquerol, K. Sing, Adsorption by Powders and Porous Solids: Principles, Methodology and Applications, Academic Press, London, 1999.
[18] K. Yamada, R. Gasparac, C.R. Martin, J. Electrochem. Soc. 151 (2004) E14.
[19] J.Y. Lee, S.M. Park, J. Electrochem. Soc. 147 (2000) 4189.
[20] S. Sadki, P. Schottland, N. Brodie, G. Sabouraud, Chem. Soc. Rev. 29 (2000) 283.
[21] B.E. Conway, J. Electrochem. Soc. 138 (1991) 1539.
[22] T. Yeu, K.M. Yin, J. Carbajal, R.E. White, J. Electrochem. Soc. 138 (1991) 2869.
[23] M.D. Levi, E. Lankri, Y. Gofer, D. Aurbach, T. Otero, J. Electrochem. Soc. 149 (2002) E204.
[24] P. Novak, W. Vielstich, J. Electrochem. Soc. 137 (1990) 1036.
[25] M.D. Levi, D. Aurbach, J. Electrochem. Soc. 149 (2002) E215.
[26] J.G. Killian, B.M. Coffey, F. Gao, T.O. Peohler, P.C. Searson, J. Electrochem. Soc. 143 (1996) 936.
[27] S.R. Sivakkumar, J.S. Oh, D.W. Kim, J. Power Sources 163 (2006) 573.
[28] S.R. Sivakkumar, D.W. Kim, J. Electrochem. Soc. 154 (2007) A134.